AAPG BULLETIN

Reevaluation of the porosity measurements under different confining pressures: A better appraisal of reservoir porosity

Lin Pan, Stuart J. Jones, Xiao Wang, Wen Guan, and Longlong Li

AAPG Bulletin published online 20 September 2018
doi: 10.1306/09181817131

Cite as: Pan, L., S. J. Jones, X. Wang, W. Guan, and L. Li, Reevaluation of the porosity measurements under different confining pressures: A better appraisal of reservoir porosity, *(in press; preliminary version published online Ahead of Print* 20 September 2018*):* AAPG Bulletin, doi: 10.1306/09181817131.

Reevaluation of the porosity measurements under different confining pressures: a better appraisal of reservoir porosity

Lin Pan[1, 2], Stuart J. Jones[3], Xiao Wang[1], Wen Guan[4], and Longlong Li[2]

[1] Key Laboratory of Tectonics and Petroleum Resources (Ministry of Education), China University of Geosciences, Wuhan, 430074, China.

[2] Department of Petroleum Engineering, China University of Geosciences, Wuhan, 430074. China.

[3] Department of Earth Sciences, Durham University, Durham, DH1 3LE, UK.

[4] Huabei Oilfield Company, SINOPEC, Zhengzhou, 450006, China.

Corresponding authors: Xiao Wang (xiao.wang@cug.edu.cn)

ACKNOWLEDGMENTS

This study was supported by the China National Science and Technology Major Projects (No. 2016ZX05006-003-001 and No. 2016ZX05014). Xiao Wang's visiting study in Durham University was supported by China Scholarship Council (No. 201406410047). The authors thank Linming Wang, Yuan Mao, Jianguo Jiang, Xiaoqiang Yuan, Wenyun Xu, Xuemei Ma, and Dianming Tang for their works in the experiments. The authors are also grateful to Dr. Barry J. Katz, Dr. Marco A. R. Ceia, and Dr. Benjamin Rendall for their constructive comments and detailed corrections.

Abstract

Porosity is one of the most important rock properties in describing hydrocarbon reservoirs. Tests on core samples provide direct and representative porosity data and the measurement of porosity at high confining pressures is recognized to correlate well with subsurface reservoir porosity. Whereas theoretical deductions of the changes and relationships of pressures, volumes, and compressibility suggest that porosity is reduced during the coring and lifting processes, the porosity measurement at elevated confining pressure does not evaluate original reservoir porosity. This theory is quantitatively validated by repeated laboratory experiments of loading and unloading on sandstone core samples. When the in-situ confining pressure is approximately 30-35 MPa (4350-5076 psi), coring and lifting would cause a porosity reduction of approximately 1.2%~1.6%, and the porosity test under high confining stress results in further porosity loss. A revised approach in calculating reservoir porosity from cored samples is proposed and can have significant implications for reserve calculations, recovery factors, and geostatistical reservoir models. The study is important for both conventional and unconventional reservoirs as it discusses a fundamental mechanism of porosity change.

1. Introduction

Porosity is an intrinsic property of reservoir rocks and indicates the storage capacity of the reservoir (Amyx et al., 1960; Jaeger et al., 2009; Schön, 2015). It is used as a primary indicator of reservoir quality to calculate hydrocarbon volume in place, and recoverable reserves (Pirson, 1977; D'Heur, 1984; Halvorsen and Hurst, 1990; Terry and Rogers, 2014). Petrophysicists use core porosity values to help calibrate porosity derived from well log data. Porosity is routinely obtained from core tests and well log interpretations, of which tests of

carefully selected core samples can provide direct and representative porosity data for subsurface reservoir evaluations (Pirson, 1963; Serra, 1983; Hearst and Nelson, 1985; Ellis and Singer, 2007; Civan, 2015). Porosity is determined by measuring the bulk volume, grain volume, and pore volume of core samples (Keelan, 1972, 1982; Hensel, 1982; Luffel and Howard, 1988; Hook, 2003; Honarpour et al., 2005). The most common porosity measurement directly uses Boyle's Law method: The gas transfer technique involves the injection and decompression of gas (He, CO_2, or N_2) into the pores of a fluid-free (vacuum), dry core sample; either the pore volume or the grain volume can be determined, depending upon the instrumentation and procedures. The measurement could be done either under low confining stress, or elevated confining stress which is representative of the reservoir effective stress conditions. It has been suggested that measurements at elevated confining stress more closely represent original reservoir porosity than measurements at zero or low confining stress (Nieto et al., 1994; American Petroleum Institute, 1998; Helle et al., 2001; Holt et al., 2003; McPhee et al., 2015). Porosity obtained at ambient condition is thought to be higher than original reservoir porosity as the pore volumes expand when the confining pressure is reduced. In oilfields when core is taken across the reservoir interval the oil tends to flow out of the oil-containing cores shortly after the coring and prior to lifting. This phenomenon occurs because the pressure outside of the core is lower than the pressure within the rock, and the pressure difference causes fluid expansion and possible pore space shrinkage, i.e. oil actively flows out (fluid expansion) and passively "squeezed out" (pore-space shrinkage). This discrepancy provokes a reevaluation of porosity changes throughout the stress variations.

In this paper, theoretical and experimental analyses are undertaken to appraise how porosity will change with differing confining pressures, volumes, and compressibilities. These changes are physically modelled and a new model is presented to better understand

how porosity changes with differing physical states and provide an improved quantitative approach to how core porosity may change with ambient conditions.

2. Theoretical deduction of porosity changes through coring to lifting

Porosity is the fraction of the volume of pores over the total volume of a rock (Equation 1), and the bulk volume (V_b) of a rock consists of the pore volumes (V_P) and rock matrix volumes (V_r) (Equation 2). Porosity change is the elastic volumetric response of porous media to variations in stress, i.e. the change in pore volume relative to bulk volume in a sample (Fatt, 1958; Brown and Korringa, 1975; Zimmerman et al., 1986; Zimmerman, 1990; Berryman, 1992; Berge, 1998).

$$\emptyset = \frac{V_P}{V_b} \tag{1}$$

$$V_b = V_P + V_r \tag{2}$$

The pressure or stress imposed on a layer of soil or rock by the weight of overlying material is defined as overburden pressure, also called lithostatic pressure, confining pressure or vertical stress (Fatt, 1953; Dobrynin, 1962). Pore pressure is the pressure of a fluid at some point within the pore system, also called fluid pressure, formation pressure, or reservoir pressure (Dickinson, 1953; Eaton, 1972). The overburden pressure (σ) and pore pressure (P) acting on the cored sandstone sample keeps decreasing through the coring and lifting process. When P and σ changes, the $-d\bar{\sigma}$ acts on the whole rock while the $-dP$ acts on the pore volumes. According to Betti's reciprocal theorem and applications (Betti, 1872; Laurent et al., 1993; Cheng, 2014), the total work done by the forces in three dimensions equals 0 in the balance state (Equation 3):

$$d\bar{\sigma}\left(\frac{\partial V_b}{\partial P}\right)_{\bar{\sigma}} dP + dP\left(\frac{\partial V_P}{\partial \bar{\sigma}}\right)_P d\bar{\sigma} = 0 \tag{3}$$

Equation 3 is simplified as Equation 4:

$$\left(\frac{\partial V_b}{\partial P}\right)_{\bar{\sigma}} = -\left(\frac{\partial V_P}{\partial \bar{\sigma}}\right)_P \tag{4}$$

Compressibility is introduced to quantify the ability of a soil or rock to reduce in volume under applied pressure (Brace, 1965; Brown and Korringa, 1975; Zimmerman et al., 1986). Given the overburden pressure and pore pressure conditions, the changes of porosity during coring and lifting can be studied by analyzing the compressibilities of the rock (core), rock matrix, and pores. The $(\bar{\sigma} - P)$ is set stable when determining the compressibilities (5):

$$d\bar{\sigma} = dP \tag{5}$$

In a homogenetic core sample, the relationship between rock matrix compressibility (C_r) and the changes of volumes is as in Equation 6:

$$\frac{dV_r}{V_r} = \frac{dV_b}{V_b} = \frac{dV_P}{V_P} = -c_r d\bar{\sigma} = -c_r dP \tag{6}$$

As the V_r, V_b, and V_P are the functions of σ and P, Equation 6 can be transformed into partial differential Equation 7:

$$\frac{1}{V_b}\left(\frac{\partial V_b}{\partial \bar{\sigma}}\right)_P d\bar{\sigma} + \frac{1}{V_b}\left(\frac{\partial V_b}{\partial P}\right)_{\bar{\sigma}} dP = \frac{1}{V_P}\left(\frac{\partial V_P}{\partial \bar{\sigma}}\right)_P d\bar{\sigma} + \frac{1}{V_P}\left(\frac{\partial V_P}{\partial P}\right)_{\bar{\sigma}} dP = -c_r d\bar{\sigma} = -c_r dP \tag{7}$$

hence:

$$\frac{1}{V_b}\left(\frac{\partial V_b}{\partial \bar{\sigma}}\right)_P + \frac{1}{V_b}\left(\frac{\partial V_b}{\partial P}\right)_{\bar{\sigma}} = \frac{1}{V_P}\left(\frac{\partial V_P}{\partial \bar{\sigma}}\right)_P + \frac{1}{V_P}\left(\frac{\partial V_P}{\partial P}\right)_{\bar{\sigma}} = -c_r \tag{8}$$

Considering the relationships in Equations 1 and 4, the elements of Equation 8 can be exchanged as Equation 9:

$$\frac{1}{V_b}\left(\frac{\partial V_b}{\partial P}\right)_{\bar{\sigma}} = -\frac{1}{V_b}\left(\frac{\partial V_P}{\partial \bar{\sigma}}\right)_P = -\frac{\emptyset}{V_P}\left(\frac{\partial V_P}{\partial \bar{\sigma}}\right)_P \tag{9}$$

Therefore:

$$c_r = \frac{\emptyset}{V_P}\left(\frac{\partial V_P}{\partial \bar{\sigma}}\right)_P - \frac{1}{V_b}\left(\frac{\partial V_P}{\partial \bar{\sigma}}\right)_P \tag{10}$$

In a constant-temperature experimental condition, the pore compressibility (c_P) can be determined by either changing the confining pressure (σ) while remaining the pore pressure (P) stable as in Equation 11:

$$c_P = -\frac{1}{V_P}\left(\frac{\partial V_P}{\partial \bar{\sigma}}\right)_P \tag{11}$$

or changing P while keeping σ stable as in Equation 12:

$$c_P = -\frac{1}{V_P}\left(\frac{\partial V_P}{\partial P}\right)_{\bar{\sigma}} \tag{12}$$

In reservoir condition, σ stays unchanged to the specific reservoir rock, whereas P decreases or increases corresponding to the expulsion or injection of fluid. In this case, the rock compressibility (c_b) and pore compressibility (c_P) are:

$$c_b = -\frac{1}{V_b}\left(\frac{\partial V_b}{\partial P}\right)_{\bar{\sigma}} \tag{13}$$

$$c_P = -\frac{1}{V_P}\left(\frac{\partial V_P}{\partial P}\right)_{\bar{\sigma}} \tag{14}$$

Combining Equations 10, 13 and 14, a new relationship of the three compressibilities can be derived:

$$c_b - c_r = \phi c_P \tag{15}$$

Defining a new intermediate function (c_f) to investigate the change of porosity:

$$c_f = \frac{1}{\phi}\left(\frac{\partial \phi}{\partial \bar{\sigma}}\right)_P \tag{16}$$

Equation 16 can be transformed combining Equations 1 and 15 as:

$$c_f = \frac{1}{\phi}\left(\frac{\partial \phi}{\partial \bar{\sigma}}\right)_P = \frac{V_b}{V_P}\left(\frac{\partial(\phi)\frac{V_P}{V_b}}{\partial \bar{\sigma}}\right)_P = c_P - c_b = \frac{1}{\phi}[c_b(1-\phi) - c_r] \tag{17}$$

Generally, c_b is more than ten times greater than c_r, thus Equation 17 can be reformed in approximate to:

$$c_f = \frac{1}{\phi} c_b (1-\phi) \tag{18}$$

A partial differential equation of porosity versus pressure can now be derived from Equations 16 and 18:

$$\left(\frac{\partial \phi}{\partial \bar{\sigma}}\right)_P = c_b(1-\phi) \tag{19}$$

The c_b of sandstones typically ranges (0.0001~0.0004)/MPa in the pressure interval of 0~40 MPa (Zimmerman, 1990). Though c_b is pressure dependent, the value of c_b in

reservoir condition is so small that its change with pressure change becomes negligible comparing to the value of $(1-\phi)$. Thus, here it can be assumed as a very small constant.

In the process of coring and lifting the core to the surface, the confining pressure of surface and reservoir is given σ_1 and σ_2, respectively ($\sigma_2 > \sigma_1$). The porosities of the two ends are correspondingly ϕ_1 and ϕ_2. The integration of ϕ in Equation 19 from σ_2 to σ_1 leads to:

$$\phi_2 = 1 - (1-\phi_1)e^{c_b(\sigma_1-\sigma_2)} \tag{20}$$

As $\sigma_2 > \sigma_1$, resulting $e^{c_b(\sigma_1-\sigma_2)} < 1$, hence $1-(1-\phi_1)e^{c_b(\sigma_1-\sigma_2)} > \phi_1$

giving the final relationship between ϕ_1 and ϕ_2 as: $\phi_2 > \phi_1$

This deduction identifies that the porosity of in-situ reservoir rock is greater than the porosity at the surface, i.e. the porosity reduces during the coring and lifting process.

3. Experimental apparatus and procedures

To verify the theoretical conclusion, we designed an apparatus to simulate the fluid activity and porosity changes through loading and unloading processes. This apparatus is primarily designed to make artificial cores that resemble reservoir rocks in composition, pore structure, and permeability. This apparatus comprises a high-pressure-high-temperature (HPHT) pump, a control system, an incubator temperature system, a compaction cylinder, a fluid expulsion acquisition system, and a data acquisition system (Figure 1). The compaction cylinder is 13 cm (~5 inch) in inner diameter, thus the cores made in this cylinder are the same size as real cores.

The experimental materials consist of 70-90 wt% matrix grains and 10-30 wt% cements. The matrix grains are river channel sand grains with the sizes of 1.0-1.2 mm, 0.55-1.0 mm, 0.50-0.55 mm, 0.43-0.50 mm, 0.38-0.43 mm, 0.27-0.38 mm 0.25-0.27 mm, 0.21-0.25 mm, 0.18-0.21 mm, 0.12-0.18 mm, 0.10-0.12 mm, 75-106 μm, 58-75 μm, 48-58 μm, 45-48 μm, 42-45 mm or 38-42 mm. The mixing and matching of these sand grains can

provide the grain matrix of coarse sandstone, medium sandstone, fine sandstone, etc. The cements consist of calcium carbonate ($CaCO_3$), magnesium carbonate ($MgCO_3$), ferrous oxide (FeO), aluminum chloride ($AlCl_3$), and clay minerals, with concentrations of 3-10%, 2-5%, 0-3%, 0-3%, and 5-15%, respectively. The materials are representative of reservoir rocks and no artificial cement is involved in the experiments. Therefore, the cements of the cores made by this method are more consistent with those of the reservoir rocks than Portland cements widely used in other artificial cores (Fattahpour et al., 2014; Trads and Lade, 2014; Li et al., 2015). In this paper, the artificial core content is 87% matrix grains and 13% cements. The matrix is mixed by 8 portions of fine-middle sand grains (0.13-0.50 mm) and 1 portion of silt grains (38-42 μm). The cements include 5% $CaCO_3$, 3% $MgCO_3$, and 5% clay minerals (Figure 2).

The matrix grains, cements, and prepared formation water (containing Mg^{2+}, Ca^{2+}, Na^+, K^+, CO_3^{2-}, Cl^-, OH^- and SO_4^{2-}) are blended and capsulated in the compaction cylinder which is placed in the incubator. Then the temperature is set and the temperature data is recorded. After the temperature stabilized, the HPHT pump starts working and pushes the piston to compact the materials. When the compaction finishes, pressure is released. The pressure data, including inlet pressure and outlet pressure (the confining pressure is the difference between inlet pressure and outlet pressure), is also recorded. During the whole experiment, the fluid expelled from the compaction cylinder is condensed, collected and measured in the measuring cup on the electronic balance. Pressure and fluid expulsion data are recorded.

Initially the temperature is set 60 °C (140 °F), and the confining pressure is 40 MPa (5800 psi). The compaction lasts 1000 min and this is defined as the first loading-stablizing stage; afterwards the temperature is lowered to room temperature and pressure is withdrawn to 0.45 MPa (65 psi), this interval is the first unloading stage; then the temperature and

pressure is elevated to 40 °C (104 °F) and 30 MPa (4350 psi), respectively, which is the second loading stage; and in the last procedure, namely the second unloading stage, the temperature and pressure are brought back to room condition. The minimum measured fluid expulsion volume in this system is 0.001 ml, and the expulsion rate in our experiment ranges between 0.001-4.42 ml/min (Table 1).

4. Experiment results

Three major factors are measured in the experiments: the confining pressure, the outlet pressure, and the volume of expelled fluid. The temperature data is also recorded in the process. The whole experiment is divided into four stages according to the settings of confining pressure and temperature (Figure 3).

4.1. Detailed analysis of experiment results:

① The first loading – stabilizing stage

At the beginning of the first loading stage the confining pressure was pumped from vacuum to 27.58 MPa (4000 psi) and the vessel was heated to 40 °C (104 °F). Fluid expulsion occurred as soon as the pressure build-up was initiated. In the next 50 minutes, the pressure and temperature were stabilized around 27.5 MPa (4000 psi) and 40 °C (104 °F), respectively. Fluid expulsion continued during this period but with much lower amplitude (0.001 ml/min). Then the pressure and temperature were raised to 38 MPa (5511 psi) and 60 °C (140 °F), respectively. The sudden increase of pressure caused a fluid expulsion jump of 0.03 ml/min. Followed by approximately 950 minutes of relatively steady pressure with subtle fluctuations. Fluid expulsion during this period was relatively stable around less than 0.001 ml/min, but several peaks can be observed and correlated with the relatively obvious changes in the pressure.

② The first unloading stage

The first unloading stage was initiated at 1000 minutes. The confining pressure

rapidly dropped to about 0.1 MPa (14.5 psi) and correspondingly the temperature was adjusted to 25 °C (77 °F). The sharp decline of pressure introduced high picks of fluid expulsion. The fluid expulsion did not cease during the first unloading stage. In this stage, the matrix grain compressibility makes the matrix grain expand and expel the fluid. The fluid near the outlet is expelled instantly, and then the fluid away from the outlet is squeezed to the outlet and expelled gradually. Fluid expansion is considered, while the value is much smaller than that of the matrix grain expansion. Matrix grain expansion is the major mechanism determining the porosity change in this stage.

③ The second loading stage

The second loading stage followed the first unloading stage. It was started by a gentle increase of confining pressure from 0.45 MPa to 1.45 MPa (65-210 psi) in 30 minutes. Fluid expulsion along with this gentle increase is subtle. Then the confining pressure was rapidly increased reaching 34 MPa (4930 psi) in 32 minutes. Fluid expulsion in this time interval exhibited significant increase and the highest instantaneous expulsion reached 4 ml/min at the starting point of rapid pressure increase.

④ The second unloading stage

The last procedure of the experiment was reducing the confining pressure to zero in 15 minutes. Fluid expulsion did not take place in the first ten minutes of this stage, but it happened afterwards. With the pressure stabilized to zero the fluid expulsion ceased.

4.2 Implications of the experimental results

The four stages in the experiment represent the different situations and processes the sandstones experienced: in-situ (the first loading – stabilizing stage), coring and lifting (the first unloading stage), lab porosity test under elevated confining pressure (the second loading stage), and the unloading after the test. The fluid expulsion is converted to porosity and correlated with the effective stress (Figure 4). The porosity had been stable and dropped only

0.6% during the fast loading and long-time stabilizing of the first loading stage, indicating the porosity is stable under constant compaction. The porosity kept decreasing mildly in the first unloading stage but the porosity loss was 1.6%, which is more obvious than the first loading stage, indicating the porosity loss during coring and lifting is not negligible. The porosity dropped sharply (3.5%) during the second loading stage, suggesting the conventional porosity test under elevated confining pressure damages the porosity significantly. The porosity loss in the second unloading stage proves the porosity damage is permanent.

5. Discussion

A model of porosity changes is established based on the theoretical analysis and experimental results (Figure 5). The nature of the porosity change is the combination of the changes of the matrix volume, grain contact, and cement relocation; it is the result of the external (confining pressure) and internal (pore pressure) forces. Rocks, as porous media, demonstrate three types of deformations: elastic, plastic, and elastic-plastic deformations (Hueckel and Maier., 1977; Mühlhaus, 2014; Grgic, 2016). Both elastic and plastic deformations take place in the loading stages (① and ③). While in the unloading stages (② and ④), a portion of elastic deformation recovers and the matrix grains expand. Theoretically the expansion of matrix grains can be in any direction, both to the exterior and to the interior, i.e. the pore spaces. However, the area of the exterior surface of a rock is smaller than the internal surface area (the total surface of the pores), making it easier for the matrix grains to expand into pore spaces. In addition, in our experiment the core is confined in the vessel leaving no room for the core to expand toward its outside. Thus, the matrix grains expand dominantly towards pore spaces. The pores are compressed and porosity is reduced. The analysis is consistent with the theoretical deduction and experimental results, which all lead to the conclusion that the porosity measured in conventional core analysis is less than that of the *in-situ* reservoir. Referring to our experimental results, for normally

compacted sandstones, when the *in-situ* confining pressure is approximately 30~35 MPa (4350-5076 psi), the coring and lifting would cause a porosity reduction of approximately 1.2%~1.6%. In this case, the porosity measurements at elevated confining stress deviate from the original porosity, thus it cannot represent the in-situ porosity without adding a proper porosity loss.

It has been suggested qualitatively that measurements at elevated confining stress more closely represent original reservoir porosity than measurements at zero or low confining stress. Our theoretical and experimental analyses indicate that porosity loss is irreversible whether the confining pressure is released or elevated. Furthermore, as physical processes act upon the core (e.g. loading or unloading) a decline in porosity will occur. Consequently, the measurement under ambient conditions shortly after coring and lifting is the best measure for reservoir porosity. Temperature is also a factor in porosity changes, however within the temperature range in our experiments (25~60 °C, i.e. 77~140 °F), the effect of temperature is not significant. Things may be more complicated at the higher temperatures and greater temperature differences, and the issue of temperature would need additional analysis.

6. Conclusion

Theoretical deductions of the changes and relationships of pressure, volume, and compressibility suggest porosities of reservoir rocks are greater at depth than at the surface due to porosity reduction during the coring and lifting process. The experiment of repeated loading and unloading of a sandstone sample quantitatively validated the theoretical analysis. When the *in-situ* confining pressure is approximately 30~35 MPa (4350-5076 psi), the coring and lifting would cause a porosity reduction of approximately 1.2%~1.6%. The original reservoir porosity should be the laboratory measured data at ambient pressure plus 1.2%~1.6%. The porosity measurement at elevated confining pressure suffers from more porosity loss and should not be used to represent the reservoir porosity. The re-consideration

of in-situ reservoir porosity by this approach demonstrates significant implications for reservoir recovery factors and reserve calculations.

Nomenclatures

V_b: the bulk volume of rock

V_p: the total volume of pores of rock

V_r: the volume of rock matrix

c_b: the bulk compressibility of rock

c_r: the compressibility of rock matrix

c_P: the compressibility of pores

σ: the overburden pressure (confining pressure)

P: the pore pressure

ϕ: porosity

Conversions for units of measurements

1 cm = 0.394 in

1 m = 3.281 ft

1 ml = 0.034 oz

1 MPa =145.038 psi

°C=(°F-32)/1.8

References

American Petroleum Institute, 1998, Recommended Practice RP 40. Recommended practices for core analysis: Washington, D.C., API Publishing Services, p. 5-15-5-17

Amyx, J. W., D. M. Bass, and R. L. Whiting, 1960, Petroleum reservoir engineering: physical properties: McGraw-Hill College, 610 p.

Berge, P., 1998, Pore compressibility in rocks, in Proceeding of the first Biot conference on poromechanics: Lauvian-la-Neuve, Belgium.

317 Berryman, J. G., 1992, Effective stress for transport properties of inhomogeneous porous
318 rock: Journal of Geophysical Research: Solid Earth, v. 97, p. 17409-17424. doi:
319 10.1029/92JB01593
320 Betti E., 1872, Teoria dell'Elasticta Nuovo Cimento Series II, VII and VIII.
321 Brace, W. F., 1965, Some new measurements of linear compressibility of rocks: Journal of
322 geophysical research, v. 70, no. 2, p.391-398. doi: 10.1029/JZ070i002p00391
323 Brown, R. J., and J. Korringa, 1975, On the dependence of the elastic properties of a porous
324 rock on the compressibility of the pore fluid: Geophysics, v. 40, no. 4, p. 608-616. doi:
325 10.1190/1.1440551
326 Cheng, A. H. D., 2014, Fundamentals of poroelasticity, in Hudson, J. A. ed., Analysis and
327 Design Methods: Comprehensive Rock Engineering: Principles, Practice and Projects,
328 p. 113-171.
329 Civan, F., 2015, Reservoir formation damage (3rd Edition): Gulf Professional Publishing,
330 1042 p.
331 D'Heur, M., 1984, Porosity and hydrocarbon distribution in the North Sea chalk reservoirs:
332 Marine and Petroleum Geology, v.1, p. 211-238. doi: 10.1016/0264-8172(84)90147-8
333 Dickinson, G., 1953, Geological aspects of abnormal reservoir pressures in Gulf Coast
334 Louisiana: AAPG Bulletin, v. 37, no. 2, p. 410-432.
335 Dobrynin, V. M., 1962, Effect of overburden pressure on some properties of sandstones:
336 Society of Petroleum Engineers Journal, v. 2, no. 4, p. 360-366. doi: 10.2118/461-PA
337 Eaton, B. A., 1972, The effect of overburden stress on geopressure prediction from well logs:
338 Journal of Petroleum Technology, v. 24, no. 08, p. 929-934. doi: 10.2118/3719-PA
339 Ellis, D. V., and J. M. Singer, 2007, Well logging for earth scientists (2nd Edition):
340 Dordrecht, Springer, 708 p.
341 Fatt, I., 1953, The effect of overburden pressure on relative permeability: Journal of

342 Petroleum Technology, v. 5, no. 10, p. 15-16. doi: 10.2118/953325-G
343 Fatt, I., 1958, Compressibility of sandstones at low to moderate pressures: AAPG Bulletin, v.
344 42, p. 1924-1957.
345 Fattahpour, V., B. A. Baudet, M. Moosavi, M. Mehranpour, and A. Ashkesari, 2014, Effect
346 of grain characteristics and cement content on the unconfined compressive strength of
347 artificial sandstones: International Journal of Rock Mechanics and Mining Sciences. doi:
348 10.1016/j.ijrmms.2014.09.008
349 Grgic, D., 2016, Constitutive modelling of the elastic–plastic, viscoplastic and damage
350 behaviour of hard porous rocks within the unified theory of inelastic flow: Acta
351 Geotechnica, v. 11, no. 1, p. 95-126. doi: 10.1007/s11440-014-0356-6
352 Halvorsen, C., and A. Hurst, 1990, Principles, practice and applications of laboratory
353 minipermeametry, in P.F. Worthington ed., Advances in Core Evaluation: Accuracy
354 and Precision in Reserves Estimation: London, Gordon and Breach Science Publishers,
355 p.521-551.
356 Hearst, J. R., and P. H. Nelson, 1985, Well logging for physical properties: New York, Mc
357 Graw-Hill Book Co, 576 p.
358 Helle, H. B., A. Bhatt, and B. Ursin, 2001, Porosity and permeability prediction from
359 wireline logs using artificial neural networks: a North Sea case study: Geophysical
360 Prospecting, v. 49, no. 4, p. 431-444. doi: 10.1046/j.1365-2478.2001.00271.x
361 Hensel, W. M., 1982, An improved summation-of-fluids porosity technique: Society of
362 Petroleum Engineers Journal, v. 22, p.193-201. doi: 10.2118/9376-PA
363 Holt, R. M., C. Lehr, C. J. Kenter, and P. Spits, 2003, In-situ porosity from cores: Poroelastic
364 correction for stress relief during coring: Petrophysics, v. 44, p. 253-261.
365 Honarpour, M., N. Djabbarah, and K. Sampath, 2005, Whole-core analysis - experience and
366 challenges: SPE Reservoir Evaluation and Engineering, v. 9, p. 460-469. doi:

10.2118/81575-MS

Hook, J. R., 2003, An introduction to porosity: Petrophysics, v.44, n. 3, p.205-212.

Hueckel, T., and G. Maier, 1977, Incremental boundary value problems in the presence of coupling of elastic and plastic deformations: a rock mechanics oriented theory: International Journal of Solids and Structures, v. 13, no. 1, p. 1-15. doi: 10.1016/0020-7683(77)90087-7

Jaeger, J. C., N. G. Cook, and R. Zimmerman, 2009, Fundamentals of rock mechanics: John Wiley & Sons, 475 p.

Keelan, D. K., 1972, Core analysis techniques and applications, in SPE Eastern Regional Meeting, Society of Petroleum Engineers. doi: 10.2118/4160-MS

Keelan, D. K., 1982, Core analysis for aid in reservoir description: Journal of Petroleum Technology, v. 34, p. 2483-2491. doi: 10.2118/10011-PA

Laurent, J., M. J. Bouteca, J. P. Sarda, and D. Bary, 1993, Pore-pressure influence in the poroelastic behavior of rocks: Experimental studies and results: SPE Formation Evaluation, v. 8, no. 2, p.117-122. doi: 10.2118/20922-PA

Li, D., X. Liu, and X. Liu, 2015, Experimental study on artificial cemented sand prepared with ordinary Portland cement with different contents. Materials, v. 8, no. 7, p. 3960-3974. http://dx.doi.org/10.3390/ma8073960

Luffel, D. L., and W. E. Howard, 1988, Reliability of laboratory measurement of porosity in tight gas sands: SPE Formation Evaluation, v. 3, p. 705-710. doi: 10.2118/16401-PA

McPhee C., J. Reed, and I. Zubizarreta, 2015, Core Analysis: A Best Practice Guide: Developments in Petroleum Science, v. 64, p. 195-211.

Mühlhaus, H. B., 2014, Continuum models for layered and blocky rock: Comprehensive rock engineering, v. 2, p. 209-231.

Nieto, J. A., D. P. Yale, and R. J. Evans, 1994, Improved methods for correcting core

porosity to reservoir conditions: The Log Analyst, v. 35, p. 21-30.

Pirson, S. J., 1963, Handbook of well log analysis for oil and gas formation evaluation: NJ. Prentice-Hall, Inc., 356 p.

Pirson, S. J., 1977, Oil reservoir engineering: RE Krieger Publishing Company, 275 p.

Schön, J. H., 2015, Physical properties of rocks: Fundamentals and principles of petrophysics (2nd Edition): Elsevier, 498 p.

Serra, O. E., 1983, Fundamentals of well-log interpretation: Elsevier, 684 p.

Terry, R. E., and J. B. Rogers, 2014, Applied petroleum reservoir engineering (3rd Edition): Prentice Hall, 528 p.

Trads, N., and P. V. Lade, 2014, Experimental evidence of truly elastic behavior of artificial sandstone inside the cementation yield surface: Rock mechanics and rock engineering, v. 47, no. 2, p.335-345. doi: 10.1007/s00603-013-0403-x

Zimmerman, R. W., 1990, Compressibility of sandstones: Elsevier, 173 p.

Zimmerman, R. W., W. H. Somerton, and M. S. King, 1986, Compressibility of porous rocks: Journal of Geophysical Research, v. 91, no. B12, p. 12765-12777.

AUTHORS

Lin Pan ~ Key Laboratory of Tectonics and Petroleum Resources (Ministry of Education), and Department of Petroleum Engineering, China University of Geosciences, Wuhan, Hubei, 430074, China; panlin@cug.edu.cn

Lin Pan is an Associate Professor in petroleum engineering at China University of Geosciences. He gained his Bachelor, Master and Doctor's degrees from China University of Geosciences in the 1990s. He has been collaborating with the industry for over 20 years. His research interests include reservoir engineering, fluid flow in porous media, CO_2 geological storage, and gas hydrates.

Stuart J. Jones ~ Department of Earth Sciences, Durham University, Durham, DH1 3LE, United Kingdom; stuart.jones@durham.ac.uk

Stuart Jones is an Associate Professor in sedimentology at Durham University. He holds a B.Sc. degree in geology from Aberystwyth University and a Ph.D. in sedimentology from the University of Reading. His research interests lie in the area of siliciclastic depositional systems and their diagenesis and, in particular, applying this to reservoir characterization.

Xiao Wang ~ Key Laboratory of Tectonics and Petroleum Resources, and Department of Petroleum Engineering, China University of Geosciences, Wuhan, Hubei, 430074, China; xiao.wang@cug.edu.cn

Xiao Wang has been working as a postdoc researcher at China University of Geosciences since 2016. She obtained her B.Sc., Master's degree and Ph.D. in petroleum geology and engineering from China University of Geosciences (2005-2016). She is interested in source rock evaluation, sandstone reservoir quality, overpressure, and geological modeling.

Wen Guan ~ Huabei Oilfield Company, SINOPEC, Zhengzhou, 450006, China.

Wen Guan is an Assistant Engineer at Hubei Oilfield Company, SINOPEC. She gained her Bachelor and Master's degree in petroleum engineering from China University of Geosciences in 2012 and 2015, respectively. Her main research interests are oil and gas field development, reservoir geology, and reserve assessment for SEC.

Longlong Li ~ Key Laboratory of Tectonics and Petroleum Resources, and Department of

442 Petroleum Engineering, China University of Geosciences, Wuhan, Hubei, 430074, China.

443 Longlong Li is a Ph.D. student in Petroleum and Gas Engineering. He received
444 bachelor's and master's degrees from China University of Geosciences in 2011 and 2014,
445 respectively. His main research directions are reservoir fluid flow, oil and gas field
446 development, reservoir physical modeling and numerical simulation.
447

448 **Figure and table captions:**

449 Figure 1. Schematic drawing of the experimental apparatus.

450 Figure 2. Photographs of the core made in this study: a. the overall image of the core which is
451 13 cm (5.12 inch) in diameter and 17 cm (6.7 inch) in length; b. the composition of
452 the core under microscope, in this image the proportions of grain matrix (mainly
453 consists of 0.13-0.50 mm quarts, feldspar, and debris), cements (clay minerals and
454 calcite), and pores are 81%, 5%, and 14%, respectively.

455 Figure 3. The details of confining pressure, temperature, and fluid expulsion in the
456 experiment. ① the first loading-stabilizing stage; ② The first unloading stage; ③
457 The second loading stage; ④ The second unloading stage.

458 Figure 4. The correlations of porosity and effective stress in the order of experimental time.
459 ① The first loading-stabilizing stage (the in-situ status); ② The first unloading
460 stage (coring and lifting); ③ The second loading stage (porosity test under high
461 confining pressure); ④ The second unloading stage.

462 Figure 5. The porosity and density of reservoir rocks in different processes.
463 ① compaction; ② coring and lifting; ③ lab porosity test under high confining
464 pressure; ④ unloading in lab test.

465 Table 1. The experiment data of pressure, temperature, and fluid expulsion.

466

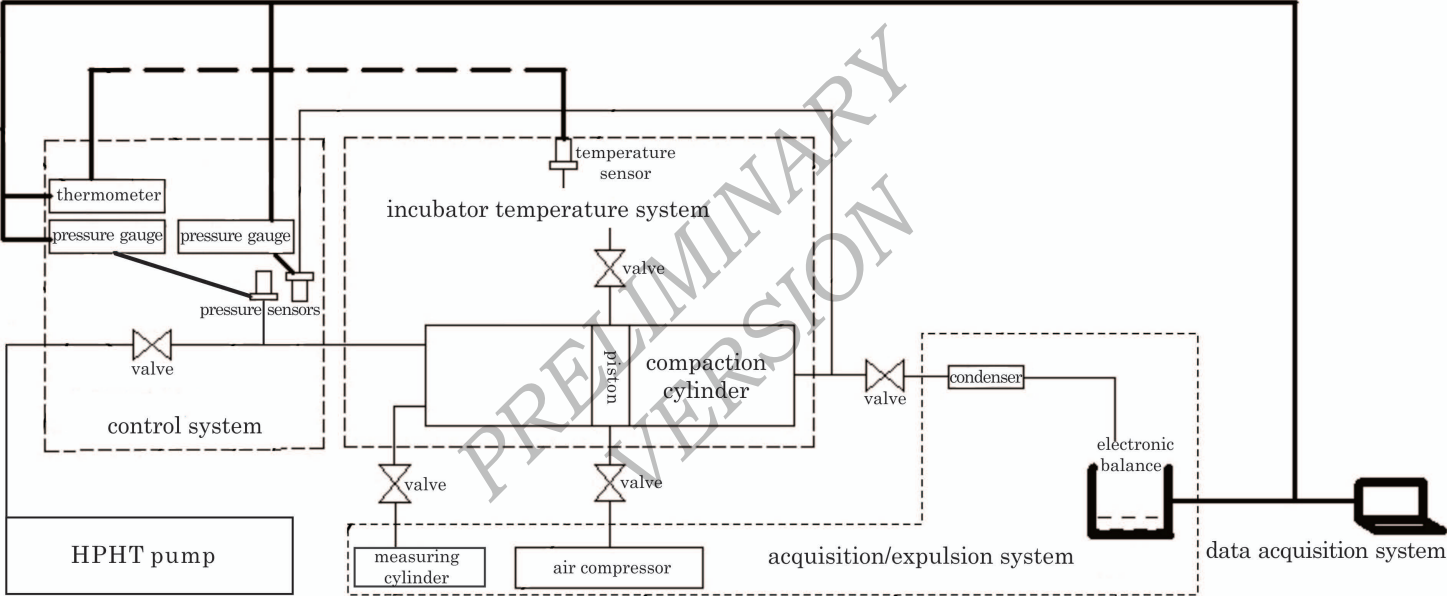
thermometer
pressure gauge
pressure gauge
pressure sensors
valve
control system
temperature sensor
incubator temperature system
valve
piston
compaction cylinder
valve
condenser
electronic balance
valve
valve
HPHT pump
measuring cylinder
air compressor
acquisition/expulsion system
data acquisition system
PRELIMINARY VERSION

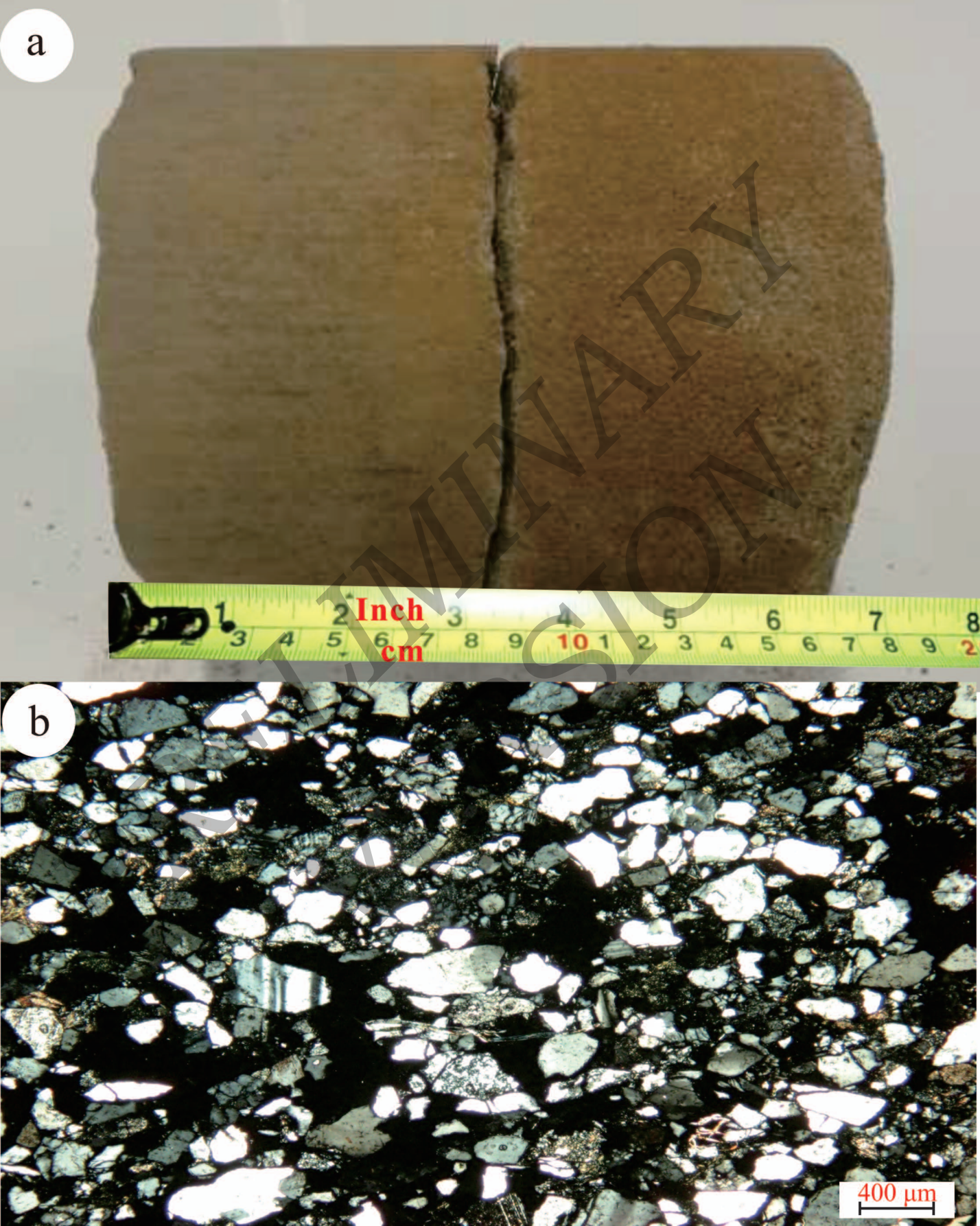

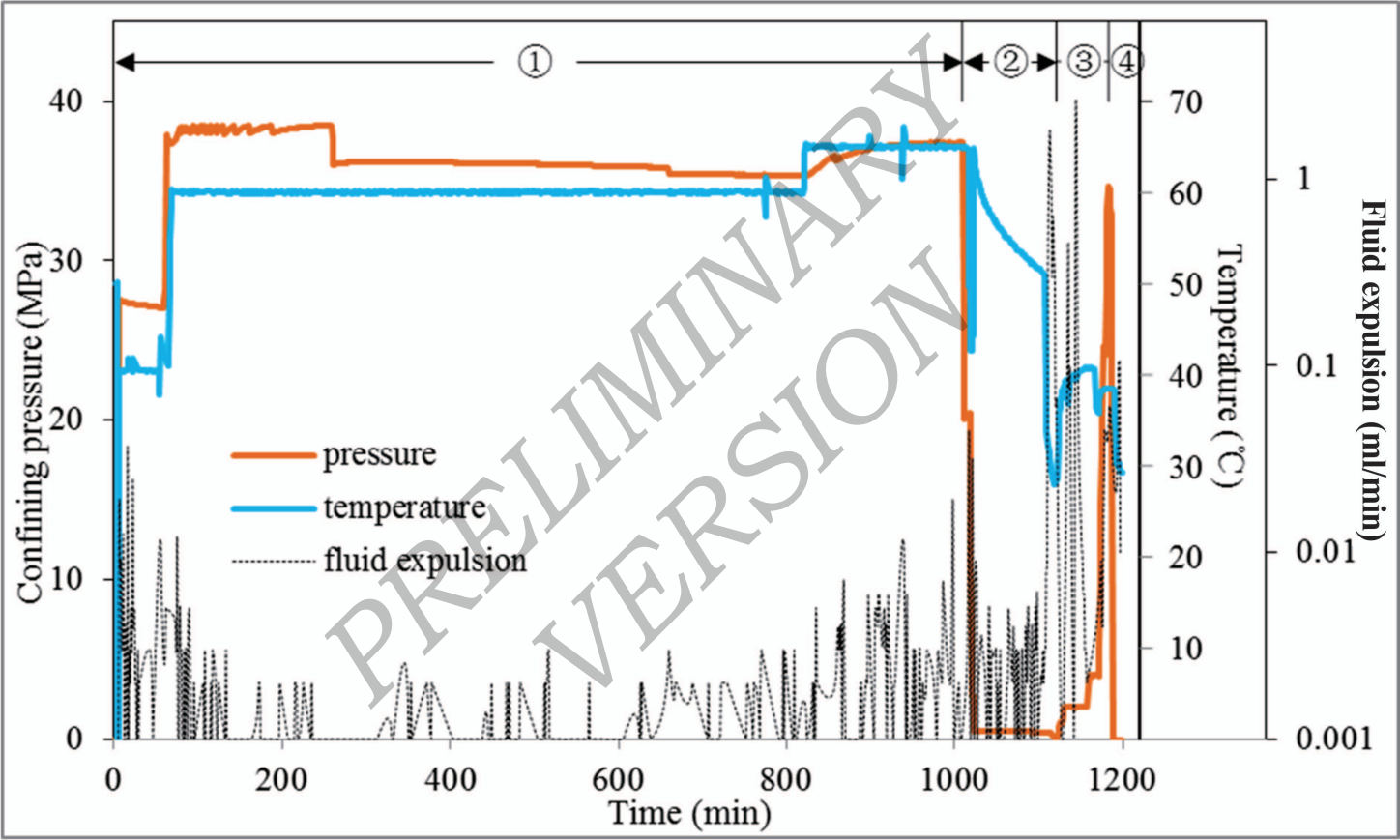
①
②
③
④
Confining pressure (MPa)
Temperature (℃)
Fluid expulsion (ml/min)
Time (min)
pressure
temperature
fluid expulsion
0
10
20
30
40
50
60
70
0.001
0.01
0.1
1
0
200
400
600
800
1000
1200
PRELIMINARY VERSION

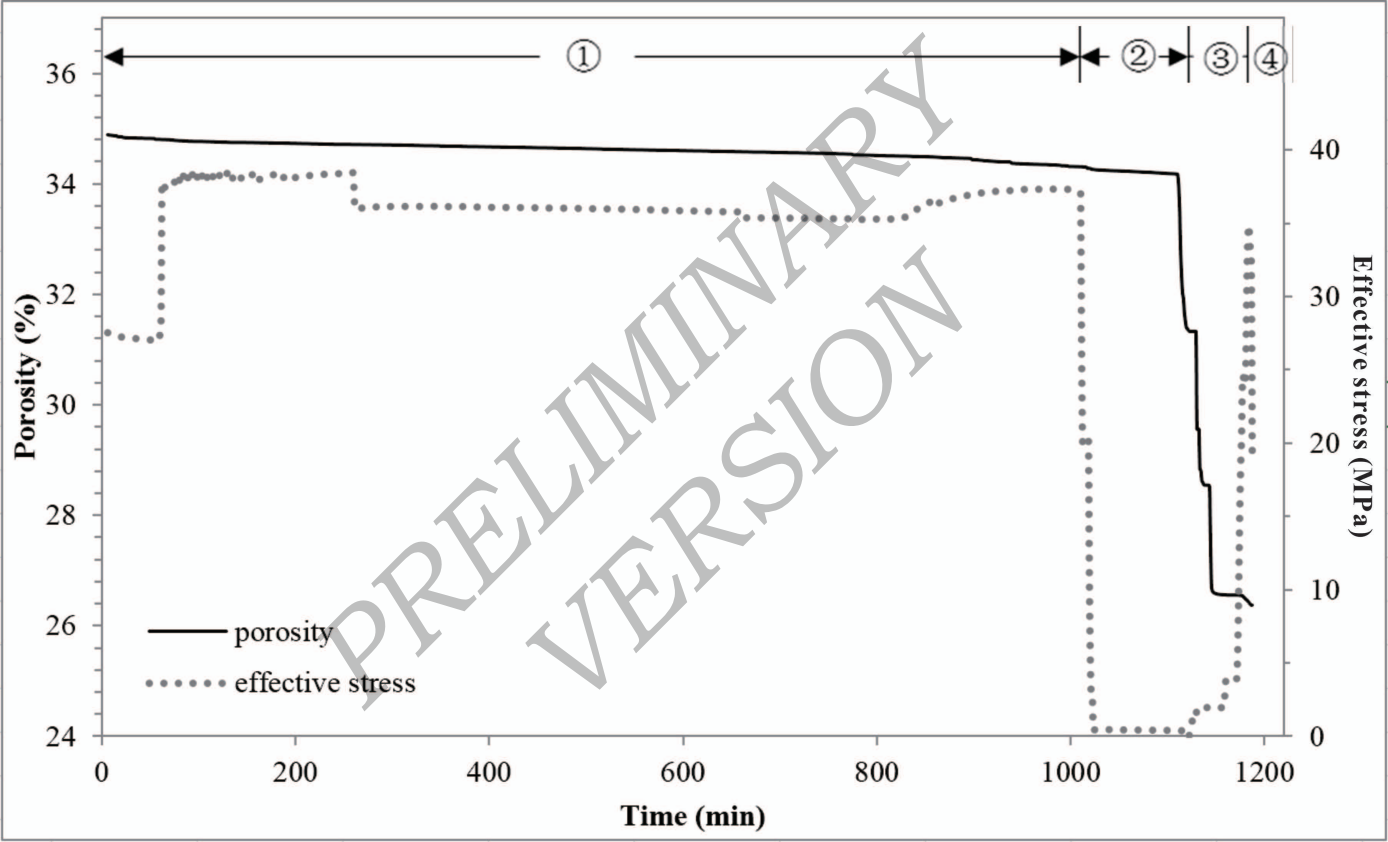
①
②
③
④
Porosity (%)
Effective stress (MPa)
Time (min)
porosity
effective stress
36
34
32
30
28
26
24
40
30
20
10
0
0
200
400
600
800
1000
1200
PRELIMINARY VERSION

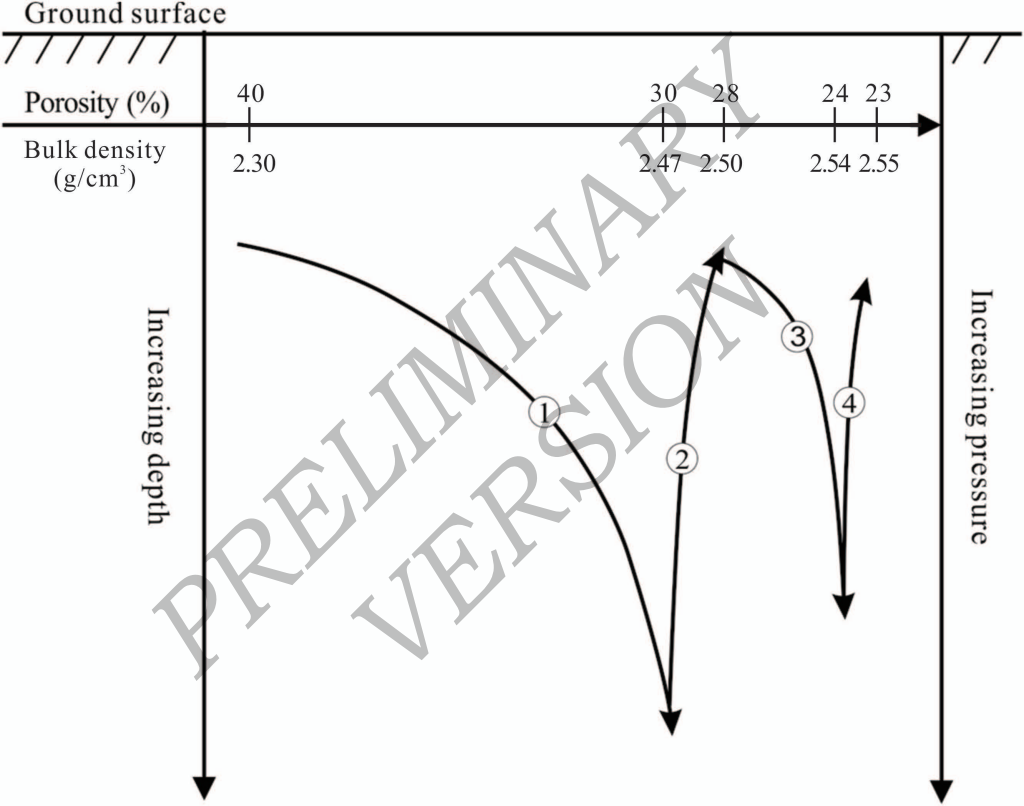

time (min)	inlet pressure (MPa)	outlet pressure (MPa)	confining pressure (MPa)	temperature (°C)	averaged fluid expulsion rate (ml/min)
10	32.81	0.04	32.77	50.20	0.003
93	38.27	0.04	38.23	60.05	0.002
206	37.24	0.04	37.20	60.05	0.001
323	36.17	0.04	36.13	60.00	0.001
434	36.08	0.04	36.04	60.00	0.001
529	35.95	0.03	35.92	60.00	0.001
636	35.61	0.04	35.58	60.10	0.001
747	35.75	0.03	35.72	62.55	0.003
848	36.79	0.03	36.76	64.95	0.003
936	37.32	0.03	37.29	65.05	0.002
949	37.36	0.03	37.33	64.95	0.002
960	37.38	0.03	37.35	64.95	0.002
976	37.39	0.03	37.36	64.95	0.003
990	37.38	0.04	37.35	64.95	0.011
1004	28.89	0.03	28.86	64.85	0.007
1017	10.45	0.04	10.42	55.65	0.022
1028	0.39	0.04	0.35	45.35	0.408
1113	0.28	0.03	0.25	29.40	1.059
1120	0.56	0.04	0.52	33.15	0.031
1129	1.72	0.04	1.69	38.30	0.050
1138	1.98	0.03	1.95	39.45	1.000
1146	1.99	0.03	1.96	40.20	0.087
1153	3.00	0.03	2.97	40.60	0.007
1161	12.24	0.03	12.21	39.50	0.005
1177	29.66	0.03	29.63	38.40	0.032
1184	17.25	0.04	17.22	34.35	1.396
1194	0.04	0.03	0.01	30.00	0.009